Environ. Sci. Technol. **2002**, *36,* 1734−1741

Reduction of Polyhalogenated Methanes by Surface-Bound Fe(II) in Aqueous Suspensions of Iron Oxides

KLAUS PECHER,*,†,‡,§
STEFAN B. HADERLEIN,§ AND
RENÉ P. SCHWARZENBACH§

University of Central Florida, Department of Physics, Orlando, Florida 32816-2385, and Swiss Federal Institute for Environmental Science and Technology (EAWAG) and Swiss Federal Institute of Technology Zurich (ETHZ), P.O. Box 611, CH-8600 Dübendorf, Switzerland

Uptake of ferrous iron from aqueous solution by iron oxides results in the formation of a variety of reactive surface species capable of reducing polyhalogenated methanes (PHMs). Pseudo-first-order reaction rate constants, k_{obs}, of PHMs increased in the order $CHBrCl_2$ < $CHBr_2Cl$ < $CHBr_3$ < CCl_4 < $CFBr_3$ < $CBrCl_3$ < CBr_2Cl_2. The k_{obs} values increased with the exposure time, t_{eq}, of Fe(II) to suspended iron oxides which was attributed to the rearrangement of initially sorbed Fe(II) species to more reactive surface species with time. At pH 7.2, the k_{obs} values of PHMs also increased with the concentration of surface-bound ferrous iron, $Fe(II)_{sorb}$, particularly when $Fe(II)_{tot}$ was increased to concentrations where surface precipitation becomes likely. At fixed total Fe(II) concentrations, k_{obs} values increased exponentially with pH. The highest reactivities were associated with pH conditions where surface precipitation of Fe(II) is expected. $Fe(II)_{sorb}$ and pH, however, had opposite effects on the product formation of PHMs. At pH 7.2, the formation of formate from CX_4 (X = Cl, Br) increased with $Fe(II)_{sorb}$, whereas increasing pH favored the formation of CHX_3. The ratio of halogenated products and formate formed is indicative of the relative importance of initial one- or two-electron-transfer processes, respectively, and was found to depend on the type of iron oxide mineral also. Our data form a basis to assess the importance of chemical reactions in natural attenuation processes of PHMs in environmental systems under iron-reducing conditions.

Introduction

In recent years, an increasing number of laboratory and field studies have demonstrated the significance of ferrous iron species in reductive transformation reactions of organic and inorganic pollutants in soils and groundwaters (for a review, see ref *1*). A common conclusion of all available studies is that ferrous iron associated with solid phases is much more reactive than Fe(II) present in dissolved form (*2*−*4*). Surface-bound Fe(II) species are also thought to play a key role in the long-term reactivity of metal iron reactive walls that are increasingly used to clean up aquifers contaminated with halogenated solvents (*5*−*9*). In contrast to the reactivity of structural Fe(II) present in certain minerals, which is generally quite low once the reactive surface sites are exhausted, the high reactivity of Fe(II) bound to iron oxide surfaces can be maintained over long time periods because such Fe(II) species may constantly be regenerated, either by sorption of Fe(II) from solution or by the activity of iron reducing microorganisms (*10*−*13*). To date, however, rather little is known about the exact nature of such iron oxide-bound Fe(II) species and about the geochemical parameters that control and modulate their formation and reactivity.

In this paper, we report the results of laboratory batch experiments on the uptake of Fe(II) from aqueous solution by various iron oxides and on the reductive transformation of a series of polyhalogenated methanes (PHMs) by such surface-bound Fe(II) species. The major goals of this study were (i) to identify and quantify important parameters that determine the type and reactivity of Fe(II) species on iron oxides, (ii) to evaluate the effects of the master variables pH and the concentration of Fe(II) on the reaction kinetics, (iii) to evaluate the effect of those variables on the mechanisms of reaction(s) with PHMs and the subsequent product formation, and (iv) to evaluate the relative reactivities of various PHMs with such surface-bound forms of Fe(II).

Materials and Methods

Iron Oxides and Chemicals. Table 1 summarizes the names and properties of the iron(hydr)oxides used in this study. All minerals were used without further pretreatment and were stored dry under lab atmosphere except for the nanohematite (*14*) which was received and stored in aqueous suspension. BET surface areas were determined by adsorption of nitrogen (Sorptomatic 1900, Carlo Erba). All iron oxides were virtually free of organic carbon contamination (f_{oc} < 0.001; CNS-analyzer EA 1108, Carlo Erba). The identity of the mineral phases was confirmed by X-ray diffraction (XRD; Siemens D 5000 and XDS 2000, Scintag, Cu Kα sources) and scanning electron microscopy (SEM; Leitz 1000 A, after sputter deposition of a thin gold layer). The chemical composition of the mineral surfaces was determined by X-ray photoelectron spectroscopy (Mg Kα-XPS, Perkin-Elmer 5400; using sample powders pressed into indium foil). No other signals than those characteristic for iron, oxygen, and adventitious carbon were present. The magnetite used gave no measurable signals of Fe(II), suggesting at least partial oxidation of its surface.

The following zwitterionic buffers (∼25 mM), also known as Good's buffers, were used for pH control: 2-(*N*-morpholino)ethanesulfonic acid monohydrate (MES), piperazine-*N*,*N*′-bis(2-ethanesulfonic acid) (PIPES), 3-(*N*-morpholino)-propanesulfonic acid (MOPS), and *N*-(2-hydroxyethyl)piperazine-*N*′-3-propanesulfonic acid (HEPPS). These buffers are known for their weak complex formation with transition metals (*15*, *16*). Anoxic ferrous iron stock solutions were prepared from $FeCl_2 \cdot 4H_2O$ (>99%, Fluka). Anoxic spike solutions of PHMs (purum, >97%) were prepared in nitrogen-purged methanol (nanograde, Burdick & Jackson). *n*-Pentane and *n*-hexane used for extraction of PHMs were PHA-grade (Promochem). All other chemicals were of p.a. quality or better. Nitrogen and N_2/H_2 gas mixtures were >99.999% (Carbagas).

Analytical Methods. PHMs and their volatile halogenated transformation products were quantified using the following

* Corresponding author phone: ++1-510-495 22 32; e-mail: khpecher@lbl.gov.
† Currently at Lawrence Berkeley National Laboratory, Advanced Light Source, MS 7-222, Berkeley, CA 94720.
‡ University of Central Florida.
§ Swiss Federal Institute for Environmental Science and Technology and Swiss Federal Institute of Technology Zurich.

10.1021/es011191o CCC: $22.00
Published on Web 03/13/2002

TABLE 1. Names, Suppliers and Characteristics of Iron(hydr)oxide Minerals Used

name (formula)	trade name (supplier)	pH_{ZPC}	BET surface ($m^2\ g^{-1}$)	$[\equiv FeOH]_t$[a] (nm^{-2})	XRD	REM	XPS
goethite (α-FeOOH)	Bayferrox 910 (Bayer AG)	7.8[b]	17.5	5.5[b,c]	√	acicular; needles with ~0.3−1.5 μm length and ~0.1 μm diameter	√
hematite (α-Fe_2O_3)	Bayferrox 105M (Bayer AG)	8.3−9.3[d]	13.7	0.7[c]	√	hexagonal platy; single crystals form larger aggregates	√
lepidocrocite (γ-FeOOH)	Bayferrox 943 (Bayer AG)	7.3[e]	17.6	1.67[e]	√	irregular plates	nd
magnetite (Fe_3O_4)	iron(II,III)oxide (Johnson & Matthey)	6.4−6.9[f]	8.1	9.4[g]	√	partly rounded octahedral crystals	oxidized[h]
hematite (α-Fe_2O_3)	nanohematite[i]	8.48	109	2.07	√	spherical particles, 10−12 nm	nd

[a] Surface site density (i.e., total number of surface hydroxyl groups per nm^2). [b] Reference *37*. [c] Reference *38*. [d] Reference *41*. [e] Reference *39*. [f] Reference *40*. [g] Calculated from ref *1*. [h] No superficial ferrous iron detected. [i] Reference *30*.

liquid−liquid microextraction GC−ECD technique. One milliliter samples for PHM analyses were withdrawn through the septum of the serum bottles containing the reaction assays using a gastight glass syringe after injection of an equal volume of nitrogen gas. A disposable luer-lock filter (0.2 μm; Spartan 3/30, Schleicher & Schüll) was placed between the needle and the syringe, and aliquots of the filtrate were immediately transferred from the syringe into crimp-sealed autosampler vials containing 0.5 mL of hexane or pentane for PHM extraction. The solvents contained $CHBr_3$ or $CHBr_2Cl$ as internal standards to correct for varying injection volumes and solvent evaporation in the subsequent GC analysis. The vials were shaken on a VORTEX mixer and were placed on a water-cooled GC autosampler rack after phase separation. Aliquots (1−2 μL) of the organic phase were withdrawn by an autosampler syringe (Fisons CTC A200S) and injected into the split/splitless injector ($T = 190$ °C; split flow ≈ 1 mL s^{-1}) of a Fisons GC 8165 equipped with a 15 m DB-624 column and an ECD detector ($T = 300$ °C; make-up gas N_2, purity 5.0; carrier gas He, purity 5.0).

The concentration raw data were corrected for losses during sampling, sample work up, and losses to the headspace of the serum vials (*17*). The accuracy of the method, including errors made during sample work up and chromatographic quantification as determined from replicate samples ($n = 8$) at two different concentrations (0.02 and 0.4 μM), was typically better than 10%.

Formate was quantified in aqueous samples using ion chromatography as described in Ammann and Rüttimann (*18*) after the oxidation of dissolved Fe(II) by atmospheric oxygen and subsequent filtration to remove Fe(III) precipitates.

The concentration of dissolved Fe(II) in suspensions of iron oxides was determined photometrically (Uvikon 930, Kontron) at 510 nm using phenanthroline as the colorimetric reagent (*19*). A sample aliquot of suspended iron oxides was withdrawn using a 1 mL polypropylene syringe and filtered through a luer-lock filter (0.2 μm; Spartan 3/30, Schleicher & Schüll) directly into a plastic cuvette containing the colorimetric assay. The method was linear from 10 μM to 1 mM dissolved Fe(II), and the precision was better than 1.2%.

Experimental Procedures. All solutions containing Fe(II) were prepared inside a glovebox (ALK 421, Coy) under anoxic conditions (atmosphere 90% N_2, 10% H_2). Control experiments conducted in pure N_2 atmosphere (*20*) showed no differences to those in N_2/H_2 mixtures. Stock solutions of Fe(II) in deoxygenated water (without pH adjustment) were stable for at least 3 weeks, as indicated by the absence of (visible) precipitates. Water (Nanopure-grade, Barnstead) was deoxygenated in 0.5 L serum bottles which were sealed with thick butyl rubber stoppers, connected to the vacuum of an aspirator via syringe needles, and heated at 120 °C in a silicon oil bath for at least 0.5 h. During cooling, the bottles were disconnected from the aspirator and purged with N_2 (Carbagas, >99.999%) for 1−2 h.

All experiments were carried out in 60 mL serum vials equipped with Teflon-coated stirring bars. Predetermined amounts of iron oxides were weighed into serum bottles, transferred to the glovebox, and filled with an aliquot of the appropriate anoxic buffer solution. The flasks were then sealed with black butyl rubber stoppers (Maagtechnic) and stirred overnight. Stirring was necessary to ensure homogeneous suspensions and to prevent aggregation of oxide particles.

Dehalogenation experiments were conducted outside of the glovebox. An aliquot of $FeCl_2$ stock solution was added through the butyl rubber stopper using a polypropylene syringe. After predetermined contact times of Fe(II) with the suspended minerals, an aliquot of a particular halogenated compound in methanolic stock solution was spiked to the suspensions using a glass syringe. The assays were constantly stirred at 600 rpm and kept in the dark at constant temperature in a water bath which was placed on a multiple stirring plate. Five to eight samples were withdrawn for PHM and product analyses over a time period covering 1−3 half-lives of the PHM studied. Vials containing halogenated compounds and Fe(II) dissolved in anoxic buffer solutions without iron oxide minerals served as controls and were kept under the same conditions.

All experiments conducted to study the interaction of dissolved ferrous iron with iron oxide minerals were carried out inside the glovebox. Sorption isotherm experiments were conducted by titrating buffered suspensions of iron oxides with a 5 mM $FeCl_2$ stock solution. Equilibration time between each addition was 36 h. The amount of Fe(II) present at the oxide surface was calculated from the concentration difference between initial and measured concentrations of Fe(II) in the filtrate.

The kinetics of Fe(II) uptake by iron oxides was examined in a similar way, but samples were withdrawn for Fe(II) analyses after varying exposure times, t_{eq}, of Fe(II) and the suspended minerals. The reversibility of the Fe(II) uptake by iron oxides was investigated with a second set of samples which were withdrawn and spiked into the phenanthroline assay without filtering. After 1 min of VORTEX shaking, these assays were filtered (0.2 μm), and the absorbance of the filtrate was measured. The difference between both sets of samples is referred to as "phenanthroline-desorbable Fe(II)".

Results and Discussions

Rate Law of PHM Reduction by Surface-Bound Fe(II). Reduction of all investigated PHMs took place in assays which

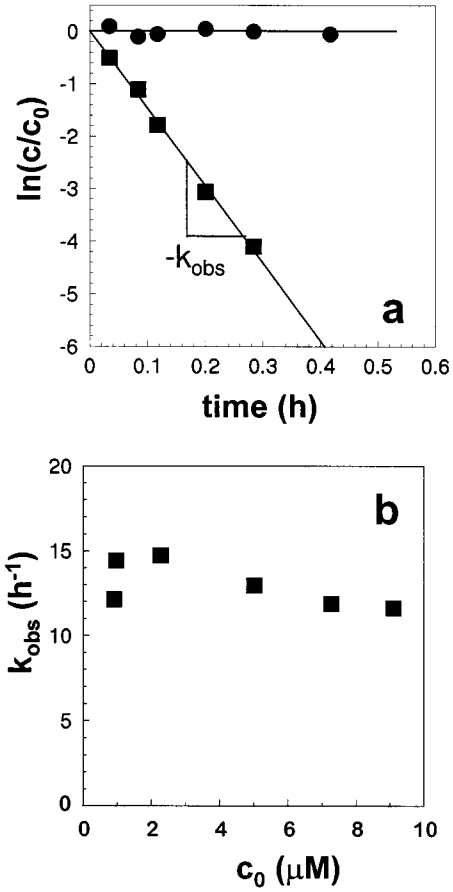

FIGURE 1. Evaluation of the rate law of the reduction of CBr_2Cl_2 by Fe(II) in suspensions of goethite (25 m^2 L^{-1}; $Fe(II)_{tot}$ = 1 mM; pH 7.2 MOPS; I = 20 mM; T = 25 °C; t_{eq}, the contact time of Fe(II) with the iron oxide before addition of PHM, was > 24 h). (a) Semilogarithmic plot of relative concentration (CBr_2Cl_2, C_0 = 2.3 μM) versus time in the presence (■) and absence of goethite (●). (b) Plot of pseudo-first-order rate constants for CBr_2Cl_2, k_{obs}, versus initial concentrations of CBr_2Cl_2 in suspension of Fe(II) and goethite.

contained both Fe(II) and iron oxide minerals. Although dissolved Fe(II) is capable thermodynamically of reducing PHMs, assays containing dissolved Fe(II) but no iron oxide minerals at circumneutral pH showed no measurable reactivity (Figure 1a). The transformation of PHMs by surface-bound Fe(II) generally followed a pseudo-first-order kinetic rate law (eq 1) as illustrated for the system CBr_2Cl_2/Fe(II)/goethite (Figure 1a).

$$\ln\left(\frac{C_t}{C_{t=0}}\right) = -k_{obs}t \qquad (1)$$

k_{obs} is an apparent pseudo-first-order rate constant for the respective halogenated compound under the prevailing conditions. In a few cases, deviations from pseudo-first-order behavior occurred with prolonged reaction times with predominantly increasing slopes for fast and decreasing slopes for slow-reacting PHMs. k_{obs} values were then obtained from the initial linear part of the $\ln(C/C_0)$ versus time plot (eq 1). The rate law of the PHM transformation was also investigated by measuring the transformation kinetics at different initial PHM concentrations. The lack of a rate dependence on the CBr_2Cl_2 concentration (Figure 1b) indicates that the pseudo-first-order approximation was reasonable for the given reaction conditions. Hence, k_{obs} values will be used for the following characterization of the reactivity of the various iron(II)/iron oxide systems. The most

TABLE 2. Names, Abbreviations, Pseudo-First-Order Rate Constants, and Half-Lives of Polyhalogenated Alkanes in Iron(II)/Goethite Suspension[a]

compound	abbreviation	k_{obs} (h^{-1})	s^b	n^c	$t_{1/2}$ (h)
bromodichloromethane	$CHBrCl_2$	0.0013	0.0002	4	533
chlorodibromomethane	$CHBr_2Cl$	0.0029	0.001	4	239
bromoform	$CHBr_3$	0.0048	0.002	2	144
tetrachloromethane	CCl_4	0.016	0.005	7	43
hexachloroethane	HCE[d]	0.0501		1	13.8
fluorotribromomethane	$CFBr_3$	0.506	0.06	2	1.37
bromotrichloromethane	$CBrCl_3$	3.577	1.52	2	0.19
dibromodichloromethane	CBr_2Cl_2	11.296	3.28	8	0.06

[a] Experimental conditions: 25 m^2 L^{-1} goethite, pH 7.2 MOPS (25 mM), t_{eq} > 24 h, $Fe(II)_{tot}$ = 1 mM. [b] Standard deviation. [c] Number of replicates. [d] t_{eq} = 5 h.

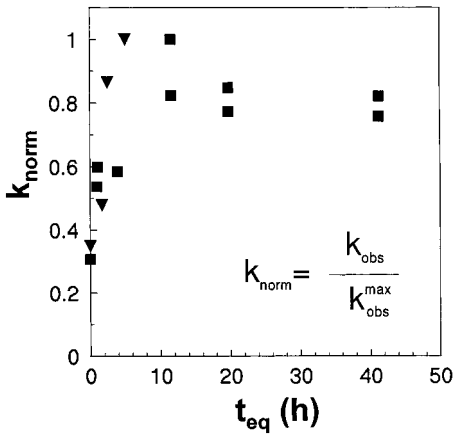

FIGURE 2. Effect of contact time (t_{eq}) of ferrous iron in suspension with goethite (25 m^2 L^{-1}) on the reduction rates of two halogenated alkanes (C_2Cl_6, C_0 = 0.4 μM (▼); and CBr_2Cl_2, C_0 = 5 μM (■)). The pseudo-first-order rate constants, k_{norm}, are normalized to the maximum apparent first-order rate constants of the respective compound (pH 7.2; $Fe(II)_{tot}$ = 1 mM; I = 20 mM; T = 25 °C).

reactive PHM, CBr_2Cl_2, (see Table 2) was preferably used to probe the reactivity of Fe(II) in the various systems at circum neutral pH. At higher pH values, CBr_2Cl_2 reacted too quickly, and k_{obs} could not be measured by our analytical method. Therefore, $CFBr_3$ was used as a probe molecule to study the effect of varying pH values on reaction kinetics. In addition to the PHMs mentioned, some data on dehalogenation kinetics of hexachloroethane (HCE) have been included.

Suspensions of goethite were used as the master system to evaluate the effects of various environmental factors on the reactivity of Fe(II) at iron oxide minerals. Experiments with other mineral oxides were performed at selected conditions to complement the goethite data.

Factors Determining the Reactivity of Fe(II) at Iron Oxide Surfaces. (1) Effect of Contact Time, t_{eq}, of Fe(II) with Suspended Iron Oxides. The reaction rates of PHMs strongly depended on the contact time of Fe(II) with the suspended iron oxides (i.e., the time allowed between addition of dissolved Fe(II) to the mineral suspension and the addition of the PHMs). Figure 2 shows normalized reaction rates, k_{norm}, for two halogenated alkanes as a function of t_{eq}. Reaction rate constants increased with increasing t_{eq} and leveled off after about 20 h of t_{eq}. A similar behavior was found for the reaction of nitroaromatic compounds in goethite/iron(II) suspensions (*21*). The strong dependence of reduction rate constants on t_{eq} during the first 20 h of exposure time of Fe(II) with iron oxides has implications both for the design of reproducible experiments as well as for the comparability of our data with those of others. Amonette et al. (*3*) used, in their study on the transformation of CCl_4 by Fe(II) in goethite

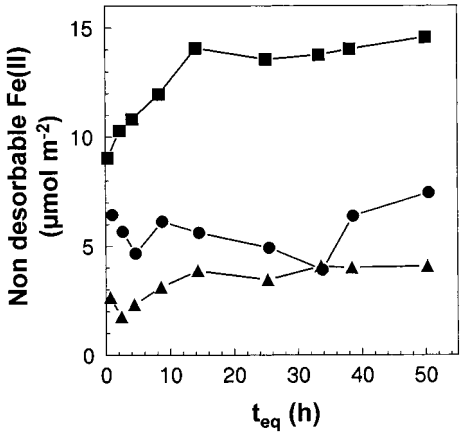

FIGURE 3. Nondesorbable surface-bound Fe(II) as a function of contact time of Fe(II) with suspended goethite (■), lepidocrocite (●), and hematite (▲) (all oxides 25 m^2 L^{-1} (pH 7.2); $Fe(II)_{tot}$ = 1 mM; I = 20 mM; T = 25 °C).

suspensions, overnight equilibration before the addition of CCl_4. In our standard experimental protocol, t_{eq} was ≥20 h in order to be able to distinguish the effects of geochemical parameters such as pH and Fe(II) content on the reactivity of the systems from the effects of nonequilibrium surface speciation of Fe(II) at iron oxides.

With respect to the distinct effect of t_{eq} on k_{obs} values, it is important to note that a time period of about 20 h was also necessary to achieve equilibrium for the uptake of Fe(II) by iron oxides. The uptake kinetics of Fe(II) by iron oxides was characterized by a fast, almost instantaneous, initial uptake phase followed by a slower second phase (*1*). Biphasic adsorption kinetics of metal cations at iron oxides have been observed previously (*22*−*24*) and can be attributed to physical (i.e., diffusion into porous minerals) or chemical processes (*25*). In our case, significant contributions of the diffusion of Fe(II) into pores can be ruled out because the goethite used is essentially nonporous (as indicated by SEM data; see supplement Figure 1 in the Supporting Information). Thus, the slow kinetics of Fe(II) uptake observed in our systems is likely due to chemical processes such as surface precipitation or formation of solid solutions. Incorporation of divalent metal cations into the superficial mineral structures of iron oxides has recently been shown to occur during aging of goethite and hematite in aqueous systems (*26*).

Coughlin and Stone (*27*) reported significant uptake of Fe(II) by goethite after 18 h, even under acidic conditions (pH 4−5.5). A large fraction of their surface-bound ferrous iron was not desorbable, even by treatment with HNO_3 for 28 h. Figure 3 shows that the amount of non-phenanthroline-desorbable Fe(II) increased with t_{eq}, particularly on goethite and less so on lepidocrocite and hematite. Phenantroline was used to extract predominantely "labile" forms of ferrous iron (i.e., Fe(II) bound by ion exchange or weak surface complexes). Thus, at pH 7.2 and a calculated surface coverage of about 60% under our experimental conditions (site densities in Table 1; effective ionic diameter of Fe^{2+} ≅ 6 Å), the formation of strongly bound ferrous iron species increased with time, consistent with a remodeling of the surface involving the formation of surface precipitates, surface clusters, or solid solutions.

Surface precipitation of ferrous iron on the iron oxide minerals used was further indicated by adsorption isotherm data (Figure 4a and data in ref *1*). The shape of the Fe(II) isotherms on goethite (and other iron oxides) is consistent with a transition from surface complexation of Fe(II) to surface precipitation or solid solution formation, which is thought to become relevant at surface saturations exceeding

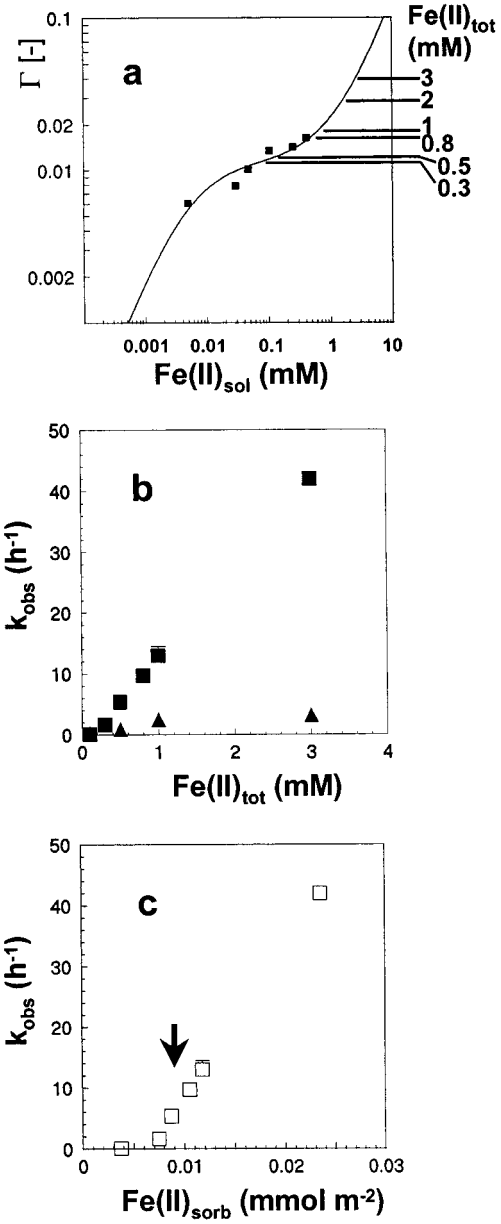

FIGURE 4. Sorption of Fe(II) at goethite and its effects on pseudo-first-order rate constants, k_{obs}, for the reduction of CBr_2Cl_2 (C_0 = 0.5 μM; 25 m^2 L^{-1} goethite (pH 7.2); I = 23 ± 3 mM; T = 25 °C). (a) Equilibrium sorption isotherm (t_{eq} ≥ 24 h, ■) and fit to the FDM-surface precipitation model (solid line); Γ = concentration of surface-bound ferrous iron per total concentration of sorbent (concentration of iron oxide participating in surface precipitation reactions + active sites for surface complexation). (b) Effects of total concentration of ferrous iron, $Fe(II)_{tot}$ and contact time, t_{eq}, of Fe(II) with suspended goethite ((▲) t_{eq} = 0 h; (■) t_{eq} > 24 h). (c) Effect of sorbed concentration of ferrous iron, $Fe(II)_{sorb}$ ((□) t_{eq} > 24 h); $Fe(II)_{sorb}$ was calculated from $Fe(II)_{tot}$ using the isotherm model of Figure 4a. The arrow denotes the total concentration of ≡Fe−OH surface sites (see Table 1).

20% (*23*). Compared to goethite, surface saturation effects by Fe(II) were even more pronounced for hematite (data not shown) because of its lower surface site density (Table 1). Modeling of Fe(II) adsorption isotherms for different oxides taking into account surface complexation and surface precipitation reactions gave a very good match between the measured data and the calculated isotherms (*1*). Compared to the simpler Langmuir model, this model allows for a continuum between the formation of single surface complexes and surface precipitation reactions (*28*) and was the

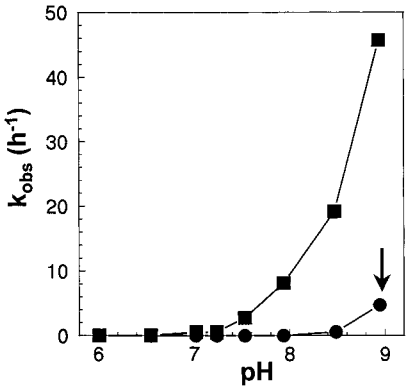

FIGURE 5. Pseudo-first-order rate constants, k_{obs}, for the transformation of $CFBr_3$ ($C_0 = 6.5\ \mu M$) in suspensions of goethite (25 $m^2\ L^{-1}$; $t_{eq} > 24$ h; $Fe(II)_{tot} = 1$ mM; $T = 25$ °C; $I = 20$ mM) as a function of solution pH (■). Also shown are k_{obs} values for the control experiments in the absence of goethite (●). The precipitate formed in the pH 8.9 control (arrow) was identified as a form of green rust (see Supporting Information, supplement Figure 2 and supplement Table 1).

only model fitting all of our sorption isotherm data (*1*). Unfortunately, isotherm modeling alone is not an absolute indicator of the type of surface species present in our systems. Additional information, preferably from in situ spectroscopic studies, is necessary to unambiguously test our hypotheses on the identity of such species. Nevertheless, the observed increase by a factor of 2−3 in the reactivity of surface-bound forms of Fe(II) with time was likely the result of rearrangement of isolated surface complexes of Fe(II) to surface clusters, solid solutions, or surface precipitates.

(2) Effect of Sorption Density of Fe(II) at Iron Oxides on k_{obs}. To evaluate the effect of surface coverage of Fe(II) on k_{obs}, experiments were conducted in which different amounts of Fe(II) were added to suspensions of goethite at otherwise constant conditions (Figure 4b). One set of experiments was performed at equilibrium conditions with respect to the uptake of Fe(II) on goethite ($t_{eq} > 24$ h), whereas the second set was conducted without previous contact of Fe(II) with the suspended goethite ($t_{eq} = 0$). A strong dependence of k_{obs} on both the total ferrous iron concentration and t_{eq} was observed. The increase of k_{obs} with increasing $Fe(II)_{tot}$ was much more pronounced for long contact times of Fe(II) with goethite ($t_{eq} > 24$ h), which further supports the hypothesis that the more reactive surface species of Fe(II) are formed after surface remodeling at the goethite surfaces.

To gain further insights into the concentration dependence of k_{obs} on Fe(II), the concentration of Fe(II) sorbed to the surface, $Fe(II)_{sorb}$, can be plotted against k_{obs} (Figure 4c). $Fe(II)_{sorb}$ was derived from the measured sorption data and the applied isotherm model. The k_{obs} values of CBr_2Cl_2 increased dramatically with $Fe(II)_{sorb}$ after saturation of the ≡FeOH surface sites was reached or exceeded (see arrow in Figure 4c).

Previous results on the transformation of CCl_4 in iron(II)/goethite suspensions (*3*) suggested a linear correlation of k_{obs} with sorbed Fe(II) concentrations at shorter contact times of Fe(II) and goethite. Our results obtained at equilibrium sorption of Fe(II) on goethite show a more complex relation between k_{obs} and $Fe(II)_{sorb}$. They demonstrate that an increase in the density of Fe(II) at the surface of the mineral (i.e., mol of Fe(II)/surface area) especially after saturation of available surface sites (i.e., the total number of ≡FeOH groups) is a crucial factor when evaluating the transformation rates of PHMs by Fe(II) in iron oxide systems.

(3) Effect of pH on k_{obs}. The effect of solution pH on the reaction rate constants of PHMs is illustrated in Figure 5 for the reduction of $CFBr_3$ in iron(II)/goethite suspensions as well as for the corresponding controls without goethite. As is evident from Figure 5, reaction rates increased almost exponentially with pH within the investigated pH range from 6 to 8.9. A similar behavior was observed by us for CCl_4 (data not shown) and somewhat less pronounced for CCl_4 by Amonette et al. (*3*). Klausen et al. (*29*) found a similar pH dependence up to pH = 8.0 for the reduction of nitrobenzene in suspensions of magnetite and Fe(II). It should be noted that, in our systems, with an increase in the pH, the concentration of $Fe(II)_{sorb}$ also increased because (i) the affinity for Fe(II) of the oxide surface increased with pH in experiments conducted at constant $Fe(II)_{tot}$ and (ii) adsorption isotherms at pH > 7 showed surface precipitation effects. Interestingly, measured or calculated adsorption edges (% sorbed vs pH) for sorption of Fe(II) on iron oxide minerals at low sorption densities (*30*, *31*) leveled off at pH > 8.0, whereas, in our system, $Fe(II)_{sorb}$ strongly increased for pH > 8 (*1*). Our data demonstrates that the surface-bound Fe(II) species formed at high pH under conditions that favor the formation of surface precipitates are more reactive than isolated surface complexes such as $\equiv FeOFe^+$ or $\equiv FeOFeOH^0$, which have been postulated at lower pH or low surface coverage (*39*).

In suspensions of goethite and Fe(II), a gradual change in color from bright yellow to blue-green was observed over the pH range from 6.0 to 8.9, suggesting the formation of mixed-valent iron phases. The SEM image of the pH 8.9 iron(II)/goethite suspension (Supporting Information, Figure 1) showed an increased surface roughness along (110) faces of the goethite needles. Thus, the observed change in color is probably due to the formation of thin surface precipitates on the goethite needles. Attempts at spectroscopic characterization of this hypothesized surface precipitate have not yet been successful. Most surface-sensitive techniques are operated at high vacuum conditions that require dry samples and, therefore, are not suited to study aqueous systems. Bulk-sensitive techniques such as scanning transmission X-ray microscopy (STXM) or XRD lack surface sensitivity and are not suited to differentiate the small amount of surface-bound Fe(II) from the bulk iron of the goethite mineral. Iron edge near-edge X-ray absorption fine structure (NEXAFS) as derived from STXM analyses gave first evidence of the existence of a surface-bound mixed-valent iron phase, however, at suspended aluminum oxide (α-Al_2O_3 (*32*)).

In this regard, it is important to note that the controls at pH 8.44 and 8.91 showed some reactivity (Figure 5), although more than an order of magnitude less than the assays containing goethite. A blue-green precipitate was observed in the pH 8.91 control, which was identified as a pure phase of green rust by XRD and SEM (Supporting Information, Table 1 and supplement Figure 2). No signals of (crystalline) $Fe(OH)_2$ were found, although the solutions at ≥ pH 8.4 were supersaturated with respect to such phases (K_{s10} ($Fe(OH)_2$(act)) = 12.85 (*33*)). Green rust is known as a powerful reductant for CCl_4 at high pH values (*2*), and its presence could, therefore, explain the observed reactivities.

In summary, the results presented so far strongly suggest that a variety of ferrous iron species coexist as potential reductants for PHMs at iron oxide surfaces. The speciation, and thus the reactivity, of these species with respect to transformation of PHMs primarily depends on the sorption density of Fe(II) at the mineral surfaces, and this, in turn, is controlled by the amount of available oxide surface, the concentration of ferrous iron in solution, the solution pH, and the contact time between dissolved Fe(II) and the oxide surfaces. The effects of these determining factors on k_{obs} were consistent for all the iron(II)/iron oxide systems studied.

Mechanistic Considerations, Product Formation, and Relative Reactivities of PHMs. From the previous discussion,

SCHEME 1

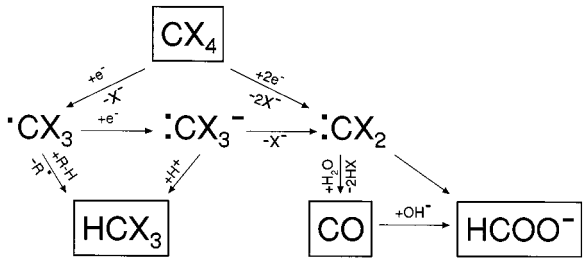

it is evident that because of the potential involvement of different forms of surface-bound Fe(II) in the reaction, the mechanisms of electron transfer to PHMs, and thus the product formation, may vary with the prevailing geochemical conditions (i.e., primarily with $Fe(II)_{sorb}$ and pH).

As is indicated by Scheme 1, the type of products formed by the reduction of PHMs with surface-bound Fe(II) is controlled by a sequence of electron-transfer reactions under the given conditions. If initial single electron-transfer processes prevail, the intermediate trihalomethane radical can abstract a hydrogen atom (e.g., from the organic buffer), leading to the accumulation of trihalomethanes in the system because these compounds react much more slowly with Fe(II) species as compared to the parent compounds (see the following discussion). If initial two-electron-transfer mechanisms prevail, either because of a simultaneous transfer of two electrons or because of two consecutive single electron-transfer steps by reaction with adjacent Fe(II) surface sites, an intermediate dihalocarbene is formed which rapidly hydrolyzes to form carbon monoxide which further reacts with H_2O to formate. Thus, an analysis of the reactivity of iron(II)/iron oxide systems in terms of electron-transfer mechanisms is useful, not only to gain further insights in the properties of the Fe(II) species involved, but also to evaluate the product formation of the reaction of Fe(II) species with PHMs. This is of great practical significance for assessing the fate of such compounds at contaminated sites.

The pH dependent protonation of a trihalocarbanion to form trihalomethanes, as speculated by Amonette et al. (*3*), can be ruled out in our systems. Experiments with CCl_2Br_2 and iron(II)/goethite performed in D_2O yielded $CHCl_2Br$ rather than $CDCl_2Br$. As all batches contained traces of methanol (from PHM stock solutions) and MOPS buffer, H-abstraction from these compounds by the trihalomethane radical is most likely. Further, the very small fraction of $CHCl_2Br$ formed in iron(II)/hematite suspensions (see Figure 9) also suggests that the protonation of trihalomethane radicals is of minor importance in such systems, at least at neutral and alkaline pH values.

Relative Reactivities and Possible Mechanisms of Electron Transfer to PHMs. The rate constants for the reactions of the 7 PHMs studied with iron(II)/goethite span a range of 4 orders of magnitude (Table 2) at the given experimental conditions. CBr_2Cl_2 was the most reactive and $CHBrCl_2$ the least reactive compound studied. The relative rate constants for the various PHMs can be compared with data obtained in homogeneous systems for which the type of electron-transfer process has been postulated (Figure 6). As can be seen from the different slopes of the regression lines shown in parts a and b of Figure 6, relative rates of PHM reduction by iron(II)/goethite at pH 7.2 resemble those obtained for mercaptojuglone as reductant, where simultaneous one- and two-electron transfer to PHMs may occur (*17*). Conversely, one-electron transfer is the only mechanism postulated in the iron(II)−porphyrine system (*34*). The comparison of the relative reactivities of the PHMs in these systems suggests that, in the iron(II)/goethite system, both one- and two-

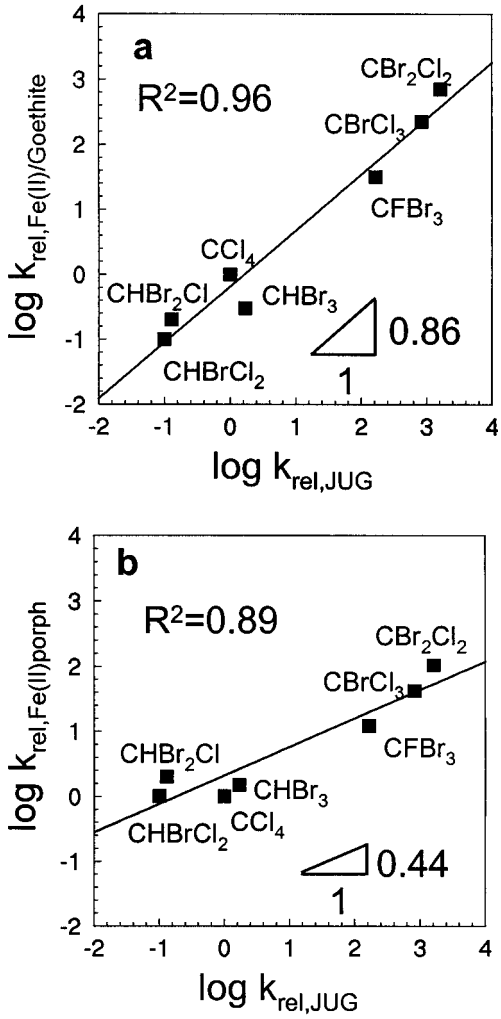

FIGURE 6. Comparison of relative rate constants log k_{rel} (normalized to CCl_4) for the reduction of PHMs by various reductants. (a) Fe(II) associated with goethite at pH 7.2 (iron(II)/goethite) and (b) dissolved iron porphyrine (Fe(II)porph) versus the hydroquinone mercaptojuglone (JUG). Data for $k_{Fe(II)porph}$ and k_{JUG} from ref *17*.

electron processes may take place in parallel at the given conditions (pH 7.2; $Fe(II)_{tot} = 1$ mM; goethite = 25 $m^2 L^{-1}$).

Products of PHM Dehalogenation. Figure 7 compares the yield of volatile halogenated products found after complete reaction of different PHMs with Fe(II) at goethite (pH 7.2; $Fe(II)_{tot} = 1$ mM; goethite 25 $m^2 L^{-1}$). A reaction was complete when either the educt was nondetectable or no more changes in its concentration occurred. The fraction trihalomethane formed (33% ± 15%) for the various compounds was fairly similar, although the reaction rates of the compounds studied varied considerably. For labeled samples shown in Figures 7 and 9, we identified 74% ± 3% of C_0 as formate in suspension of goethite and 68% ± 3% of C_0 in suspension of hematite (Bayferrox 105M). Thus, within the error margins of the analytical methods, the mass balance for the transformation of CBr_2Cl_2 in iron(II)/goethite suspensions was complete, considering $CHBrCl_2$ and formate as the only products (see Scheme 1). Because the hydrolysis rate of CO in homogeneous systems is slower than that of dichlorocarbene (*35*, *36*), carbon monoxide might have accumulated in our systems. CO may account for the incomplete mass balance found in the hematite sample, which was analyzed for PHMs, trihalomethanes, and formate but not for CO.

The data shown in Figure 7 support the hypothesis that both initial one- and two-electron-transfer processes oc-

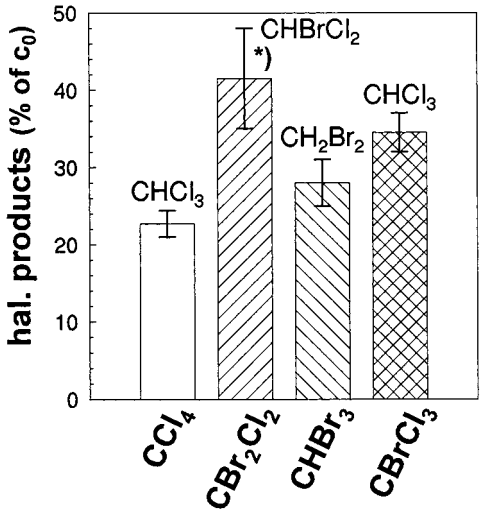

FIGURE 7. Percentage of extractable halogenated products formed after completion of the reaction of Fe(II) with different polyhalogenated methanes in suspensions of goethite (25 m^2 L^{-1}; $Fe(II)_{tot}$ = 1 mM; t_{eq} > 24 h; pH 7.2; T = 25 °C; C_0 = 1−20 μM): (*) indicates samples for which formate has been quantified.

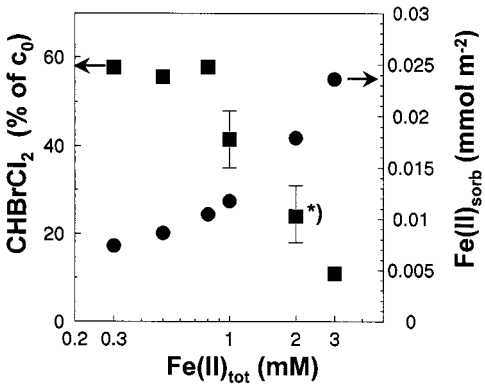

FIGURE 8. Effect of concentration of ferrous iron ($Fe(II)_{tot}$ (■) and $Fe(II)_{sorb}$ (●)) in suspension of goethite on the yield of $CHBrCl_2$ from reduction of CBr_2Cl_2 (C_0 = 1−10 μM) (25 m^2 L^{-1} goethite; t_{eq} > 24 h; pH 7.2; T = 25 °C; error bars represent ±2 SD): (*) 74% of C_0 were identified as formate in this sample.

curred simultaneously in the iron(II)/goethite system at the given conditions. Further, the data show that the mechanism of electron transfer is essentially independent of the magnitude of the reaction rates as the relative reactivity of the various PHMs shown varied by more than 3 orders of magnitude. Thus, at the given conditions, the relative importance of one- an two-electron-transfer reactions only depended on the composition of the Fe(II) surface species.

Factors Affecting Electron-Transfer Mechanisms and PHM Product Formation. The concentration of surface-bound Fe(II) affected not only the rate but also the relative importance of one- or two-electron-transfer processes and, thus, the product formation of PHMs. The yield of the one-electron-transfer product $CHBrCl_2$ decreased with increasing concentration of $Fe(II)_{sorb}$ (Figure 8). The mass balance was checked for the labeled sample in Figure 8 and was found to be made up to 100% by formate within the error margins of our analytical techniques. Thus, at pH 7.2, with increasing density of surface-bound Fe(II), the two-electron pathway with subsequent formation of CO and formate as final products predominated. This is of particular importance regarding the fate of PHMs at contaminated sites as it opens new perspectives to avoid the formation of harmful halogenated reaction products.

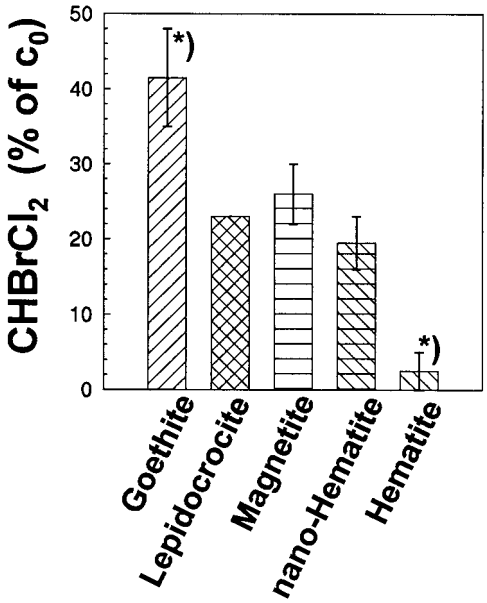

FIGURE 9. Effect of different iron oxides on the yield of $CHBrCl_2$ formed from the reduction of CBr_2Cl_2 (C_0 = 1−10 μM) by surface-bound Fe(II) (1 mM $Fe(II)_{tot}$; 25 m^2 L^{-1} oxides; t_{eq} > 24 h; pH 7.2; T = 25 °C; error bars represent ±2 SD): (*) indicates samples for which formate has been quantified.

An increase of pH also leads to higher $Fe(II)_{sorb}$ concentrations on iron oxides. The one-electron-transfer pathway, however, predominated at alkaline pH values in the iron(II)/goethite system (data not shown). Consequently, both the concentration of $Fe(II)_{sorb}$ and the pH value of an iron(II)/iron oxide system must be known to predict the product formation. The predominance of the one-electron-transfer pathway at high pH values can be rationalized by the spatial arrangements of Fe(II) and Fe(III) centers (i.e., the lack of neighboring Fe(II) sites) in green rust-like surface precipitates which are likely to form under such conditions. In a recent study on the reduction of CCl_4 by green rust, $CHCl_3$ was the major product (*2*).

Finally, the type of iron oxide mineral also had a marked influence on the predominance of one- or two-electron pathways the systems. Although the amount of surface area was held constant for each mineral, the yields of trihalomethane products for reductive transformation of CBr_2Cl_2 varied considerably among the various iron oxides studied and even among different preparations of the same type of mineral (hematite vs nanohematite in Figure 9). The observed variations among the various minerals, however, are not too surprising, considering the fact that the surface site density of ≡FeOH groups and thus the surface coverage by Fe(II) varied significantly among the various minerals for the given conditions.

Environmental Significance

Our results demonstrate that ferrous iron bound to the surface of iron oxide minerals is capable of reducing a variety of polyhalogenated methanes at appreciable rates under conditions that can be encountered in ferrogenic aquifers. The reactivity of the surface-bound Fe(II) and the type of products formed for the reaction with a given PHM vary with respect to the species formed by Fe(II) on the oxide surface upon its uptake from aqueous solution.

Although our present knowledge of the identity of reactive Fe(II) species on a molecular level is still very limited because of the lack of spectroscopic data, the results of our study may already be applicable for practical purposes (e.g., to assess and optimize natural attenuation processes of PHMs in

contaminated groundwaters). The contribution of abiotic transformation processes to the natural attenuation of PHMs in the subsurface has largely been neglected in the past. Thus, the elucidation of $Fe(II)_{sorb}$ and solution pH as master variables that control reaction rates and product distribution of PHM transformation may stimulate attempts to manipulate the condition at contaminated sites in a way that the rates of natural attenuation by reaction with surface-bound forms of Fe(II) are enhanced and the formation of harmless products is favored. Such investigations are currently in progress in our laboratory at EAWAG/ETHZ.

Furthermore, our results demonstrate the need for the development and application of surface-sensitive in-situ spectroscopic techniques that allow us to study heterogeneous Fe(II)/Fe(III) systems in the presence of water. In this regard, STXM is a very promising approach that will be further developed at the Advanced Light Source in Berkeley to elucidate the structure of reactive Fe(II) species at mineral oxides.

Acknowledgments

C. Drummer (BIMF, Bayreuth (D)) and K.-H. Ernst (EMPA, Dübendorf (CH)) are gratefully acknowledged for their help with the SEM imaging and XPS measurements. A. Amman (EAWAG) conducted the analysis of formate, and D. Christl performed most of the Fe(II) adsorption experiments. T. Waxweiler developed most of the analytical methods and contributed experimental data on reduction of HCE. Colloidal hematite (referred to as nanohematite) was kindly provided by L. Charlet, Nancy (F). We also thank C. Eggleston, U. von Gunten, M. Elsner, A. Kappler, J. Klausen, S. Hug, and D. McCubbery for reviewing the manuscript. The insightful and competent comments of three anonymous reviewers greatly improved the presentation of this work. This work was partially funded by DFG (Grant Pe 581/1-1) and the DOW Foundation Supporting Public Health and Environmental Research Efforts (SPHERE) program.

Supporting Information Available

SEM and XRD data. This material is available free of charge via the Internet at http://pubs.acs.org.

Literature Cited

(1) Haderlein, S. B.; Pecher, K. Pollutant reduction in heterogeneous Fe(II)/Fe(III) systems. In *Kinetics and Mechanisms of Reactions at the Mineral/Water Interface, ACS Symposium Series, Division of Geochemistry*; Sparks, D. L., Grundl, T., Eds.; American Chemical Society: Washington, DC, 1998; Vol. 715, Chapter 17, pp 342−357.
(2) Erbs, M.; Hansen, H. C. B.; Olsen, C. E. *Environ. Sci. Technol.* **1999**, *33*, 307−311.
(3) Amonette, J.; Workman, D. J.; Kennedy, D. W.; Fruchter, J. S.; Gorbi, Y. A. *Environ. Sci. Technol.* **2000**, *34*, 4606−4613.
(4) Hwang, I.; Batchelor, B. *Environ. Sci. Technol.* **2000**, *34*, 5017−5022.
(5) Johnson, T. L.; Fish, W.; Gorby, Y. A.; Tratnyek, P. G. *J. Contam. Hydrol.* **1998**, *29*, 379−398.
(6) Deng, B.; Campbell, T. J.; Burris, D. R. *Environ. Sci. Technol.* **1997**, *31*, 1185−1190.
(7) Scherer, M. M.; Balko, B. A.; Tratnyek, P. G. The role of oxides in reduction reactions at the metal−water interface. In *Kinetics and Mechanisms of Reactions at the Mineral/Water Interface, ACS Symposium Series, Division of Geochemistry*; Sparks, D. L., Grundl, T., Eds.; American Chemical Society: Washington, DC, 1998; Vol. 715, Chapter 15, pp 301−322.
(8) Bonin, P. M. L.; Jedral, W.; Odziemkowski, M. S.; Gillham, R. W. *Corros. Sci.* **2000**, 1921−1939.
(9) Balko, B. A.; Tratnyek, P. G. *J. Phys. Chem.* **1998**, *101*, 1459−1465.
(10) Heijman, C. G.; Grieder, E.; Holliger, C.; Schwarzenbach, R. P. *Environ. Sci. Technol.* **1995**, *29*, 775−783.
(11) Roden, E. E.; Zachara, J. M. *Environ. Sci. Technol.* **1996**, *30*, 1618−1628.
(12) Hofstetter, T. B.; Heijman, C. G.; Haderlein, S. B.; Holliger, C.; Schwarzenbach, R. P. *Environ. Sci. Technol.* **1999**, *33*, 1479−1487.
(13) Urrutia, M. M.; Roden, E. E.; Fredrickson, J. K.; Zachara, J. M. *Geomicrobiol. J.* **1998**, *15*, 269−291.
(14) Charlet, L.; Liger, E.; Gerasimo, P. *J. Environ. Eng.* **1998**, *124*, 25−30.
(15) Yu, Q.; Kandegedara, A.; Xu, Y.; Rorabacher, D. B. *Anal. Biochem.* **1997**, *253*, 550−556.
(16) Perrin, D. D.; Dempsey, B. Buffers for pH and metal ion control.; Chapman and Hall: London, U.K., 1974.
(17) Perlinger, J. A.; Buschmann, J.; Angst, W.; Schwarzenbach, R. P. *Environ. Sci. Technol.* **1998**, *32*, 2431−2437.
(18) Ammann, A. A.; Rüttimann, T. B. *J. Chromatogr. A* **1995**, *706*, 259−269.
(19) Frevert, T. Hydrochemisches Grundpraktikum.; UTB: Stuttgart, Germany, 1983.
(20) Elsner, M. Personal communication.
(21) Rügge, K.; Hofstetter, T. B.; Haderlein, S. B.; Bjerg, P. L.; Knudsen, S.; Zraunig, C.; Mosbæk, H.; Christensen, T. H. *Environ. Sci. Technol.* **1998**, *32*, 23−31.
(22) Kinniburgh, D. G.; Jackson, M. L. Cation adsorption by hydrous metal oxides and clays. In *Adsorption of inorganics at solid−liquid interfaces*; Anderson, A. A., Rubin, A. J., Eds.; Ann Arbor Science: Newton, MA, 1981; Vol. 3, pp 91−160.
(23) Dzombak, D. A.; Morel, F. M. M. Surface complexation modeling. Hydrous ferric oxide.; John Wiley and Sons: New York, 1990.
(24) Sposito, G. Distinguishing adsorption from surface precipitation. In *Geochemical processes at mineral surfaces, ACS Symposium Series 323*; Davis, J. A., Hayes, K. F., Eds.; American Chemical Society: Washington, DC, 1986; Vol. 11, pp 217−228.
(25) Hachiya, K.; Sasaki, M.; Ikeda, T.; Mikami, N.; Yasunaga, T. *J. Phys. Chem.* **1984**, *88*, 27−31.
(26) Ford, R. G.; Bertsch, P. M.; Farley, K. J. *Environ. Sci. Technol.* **1997**, *31*, 2028−2033.
(27) Coughlin, B. R.; Stone, A. T. *Environ. Sci. Technol.* **1995**, *29*, 2445−2455.
(28) Farley, K. J.; Dzombak, D. A.; Morel, F. M. M. *J. Colloid Interface Sci.* **1985**, *106*, 226−242.
(29) Klausen, J.; Tröber, S. P.; Haderlein, S. B.; Schwarzenbach, R. P. *Environ. Sci. Technol.* **1995**, *29*, 2396−2404.
(30) Liger, E.; Charlet, L.; Van Cappellen, P. *Geochem. Cosmoch. Acta* **1999**, *63*, 2939−2955.
(31) Zachara, J. M.; Smith, S. C.; Frederickson, J. K. *Geochem. Cosmoch. Acta* **2000**, *64*, 1345−1362.
(32) Pecher, K.; Kneedler, E.; McCubbery, D.; Meigs, G.; Tonner, B. *ACS, Division of Environ. Chem., Preprints of Extended Abstracts* **2000**, *40* (2), 323−325.
(33) Baes, C. F., Jr.; Mesmer, R. E. The hydrolysis of cations.; John Wiley and Sons: New York, 1976.
(34) Buschmann, J.; Angst, W.; Schwarzenbach, R. P. *Environ. Sci. Technol.* **1999**, *33*, 1015−1020.
(35) Pliego, J. R., Jr.; de Almeida, W. B. *J. Phys. Chem.* **1996**, *100*, 12410−12413.
(36) Robinson, E. A. *J. Chem. Soc.* **1961**, 1663−1671.
(37) Müller, B. Über die Adsorption von Metallionen an Oberflächen aquatischer Partikel.; Diss. ETH Nr 8988: Zürich, Switzerland, 1989.
(38) Ruf, A. Reduktive Auflösung von Eisen(hydr)oxiden durch Ascorbat und Hydrochinone.; Diss. ETH Nr 9892: Zürich, Switzerland, 1992.
(39) Zhang, Y.; Charlet, L.; Schindler, P. W. *Colloids Surf.* **1992**, *63*, 259−268.
(40) Regazzoni, A. E.; Blesa, M. A.; Maroto, A. J. G. *J. Colloid Interface Sci.* **1983**, *91*, 560−570.
(41) Parks, G. A. *Chem. Rev.* **1965**, *65*, 177−198.
(42) McGill, I. R.; McEnaney, B.; Smith, D. C. *Nature* **1976**, *259*, 200−201.
(43) Miyamoto, H. *Mater. Res. Bull.* **1976**, *11*, 329−336.

Received for review August 3, 2001. Revised manuscript received January 30, 2002. Accepted February 11, 2002.

ES011191O